

# Solvent Effect on the Curing of Polyimide Resins

TZU-CHIEN J. HSU\* and ZU-LING LIU

Institute of Materials Science and Engineering, National Sun Yat-Sen University,  
Kaohsiung 804, Taiwan, Republic of China

## SYNOPSIS

The effect of the solvent 1-methyl-2-pyrrolidinone (NMP) on the curing of polyimide resins synthesized from pyromellitic dianhydride (PMDA) and 4,4'-oxydianiline (ODA) has been investigated. Three polyimide precursors, i.e., the polyamic acid (PAA), with controlled amount of NMP were prepared. The study was aimed first to independently investigate the decomplexation process, which involved the evolution of hydrogen-bonded NMP from PAA, without interference from imidization. This was accomplished by TGA at varying heating rates using different solvent content in PAA. The observed one-stage decomplexation process suggested that the complex formation of NMP and PAA was not the same as the model compound studied by others. An average value of 150 kJ/mol for the activation energy of the decomplexation process was obtained. The study then sought to identify the effect of the decomplexation on the imidization kinetics by employing DSC at several drying temperatures and also varying heating rates. This allowed one to control the extent of plasticization that occurred to facilitate the imidization process. Our DSC data showed that over-drying PAA resulted in prolonged imidization due mainly to the lack of plasticization by decomplexed NMP. The estimated enthalpy of imidization and that of decomplexation were 114 kJ/mol and 53 kJ/mol NMP, respectively. Finally, the imidization kinetics was independently investigated using FTIR, without the interference from decomplexation process. The results indicated that there were four stages during the entire imidization process. Up to a temperature of 150°C, less than 20% of amide groups had reacted to give imide groups and the reaction was slow. Most of the imidization took place between 150 and 180°C with conversion as high as 90%. The imidization process was completed after the temperature was further raised to 250°C. Above 250°C, the reverse reaction became more significant (due probably to configurational and packing preference) and resulted in a lowering of final conversion back to 80%. © 1992 John Wiley & Sons, Inc.

## INTRODUCTION

In recent years there has been increasing interest in polyimide resins in the aerospace and electronic industries.<sup>1,2</sup> This is mainly due to their outstanding properties such as excellent mechanical strength, high thermal stability, and good electrical properties.

Synthesis of an aromatic polyimide is usually performed by a two-stage method. The first step involves acylation of a diamine with a tetraacid dianhydride in a polar solvent to form a soluble polyamic acid (PAA), a precursor of the polyimide. The sec-

ond step involves the dehydrative cyclization of the PAA (imidization) to give rise to the polyimide (PI). This description fails to disclose the complexity and specific features of the two-step method. Important factors that affect the ultimate properties of a polyimide resin may include the nature of solvent-PAA interaction, the imidization reaction, and the side reactions accompanying these processes such as the reversible anhydride formation.

The solvent-PAA interaction has been well established by various authors.<sup>3-6</sup> Worthy of note is the study of a low-molecular-weight polyimide model compound by Brekner and Feger.<sup>3</sup> They revealed the existence of 4/1 and 2/1 molar complexes between the solvent 1-methyl-2-pyrrolidinone (NMP) and the diamic acid synthesized from pyromellitic

\* To whom correspondence should be addressed.

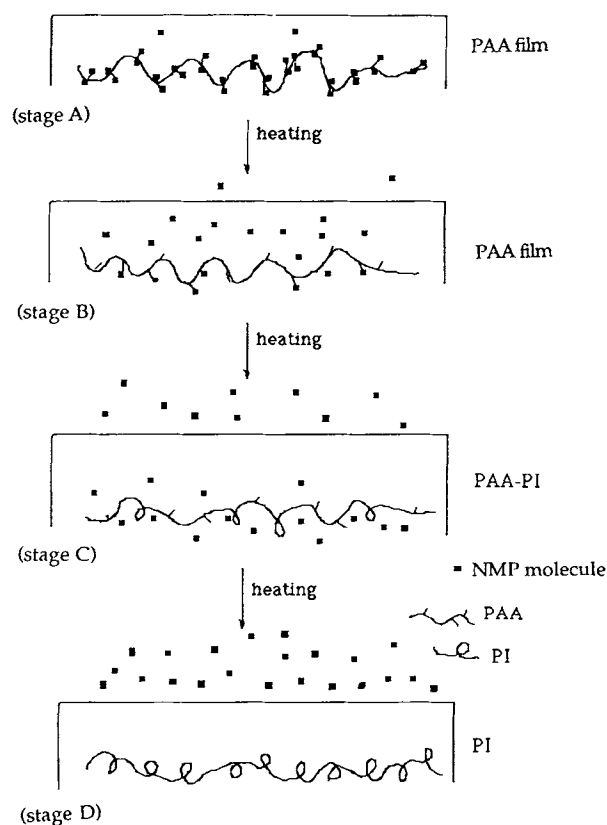


**Figure 1** Schematic illustrating the evolution of NMP from polyamic acid solution.

dianhydride (PMDA) and aniline. Figure 1 illustrates schematically the occurrence of the solvent evaporation (decomplexation) and the thermal imidization during the cure of polyimide resin, both strongly affected by the external heat input.

The results on the study of model compounds have been extended to the PAA molecule.<sup>4</sup> In addition to the four NMP molecules hydrogen bonded to the PAA molecules, there are also free NMP molecules in the solid PAA film (stage A, Fig. 1). Once decomplexed, these free NMP molecules help to plasticize the PAA film and thus should facilitate the imidization during cure as the curing temperature is raised. Eventually, they evaporate out of the film. Meanwhile, the H-bonded NMP molecules have different energy barriers to leave the PAA molecule. The two NMP molecules H-bonded to amide moiety will decomplex first since they have lower decomplexation energy compared to the other two NMP molecules attached to acid moiety (50 vs. 87 kJ/mol NMP, stage B in Fig. 1).<sup>3</sup> Once decomplexed, they can plasticize the PAA film before leaving the film. At the same time, part of the amide groups have reacted to give imide groups. In addition,

it has been reported that anhydride formation, a reversible degradation of the molecular weight of amic acid, is a side reaction competing with the imidization.<sup>3</sup> As the temperature further increases (stage C, Fig. 1), the other two NMP molecules H-bonded to carboxylic acid moiety become decomplexed and the PAA film is plasticized. Most of the imidization takes place during this stage. Finally, further heating allows NMP to leave the film completely and solvent-free polyimide film is obtained (stage D, Fig. 1).

The duration of solvent in the PAA film (plasticization) depends on the rate of decomplexation. As a result, a low heating rate should promote the effect of the plasticization. Note that thermal imidization cannot start before decomplexation takes place. On the other hand, a higher heating rate is preferred from the viewpoint of thermal imidization. Consequently, there must exist an optimum heating rate that allows decomplexation, plasticization, and imidization to balance each other to result in a polyimide film of desired ultimate physical or mechanical properties.

Even though many facts are known, especially in the model compound, a comprehensive understanding of the solvent-PAA interactions in the formation of the polyimide is still unknown. The main objective of this work is to further explore the solvent-PAA interactions in the polyimide resin. The experimental designs are aimed first to study the decomplexation process, independent of the imidization. This is done by using thermogravimetric analysis (TGA). The solvent-PAA interactions are further studied by differential scanning calorimetry (DSC) in detail, taking into account both the decomplexation and imidization processes. Finally, the imidization kinetics are investigated using Fourier transform infrared spectroscopy (FTIR), independent of the decomplexation process.

## EXPERIMENTAL

### Synthesis of Polyamic Acid

The materials used in this study included pyromellitic dianhydride (PMDA, from TCI) and 4,4'-oxydianiline (ODA, from TCI). PMDA was dried at 150°C for 24 h prior to synthesis. ODA (0.03 mol) was first dissolved in 70 mL of 1-methyl-2-pyrrolidinone (NMP, from Janssen) in a 500-mL 3-neck round flask with a slow current of dry nitrogen passing over the liquid. The solution was cooled to 10°C, until dissolution was complete. The synthesis of PAA was carried out by slowly adding PMDA (0.03 mol) to the solution in approximately four equal

portions while stirring at 10°C. Time was allowed for each addition for complete reaction, indicated by disappearance of all solid particles. This took about 5–6 h. The viscous PAA solution so obtained (NMP/PI = 23.3 molar ratio) was then sealed with nitrogen gas and kept refrigerated at 4°C until further use.

### Solvent Removal

Table I lists three PAA samples with different contents of NMP prepared in this study. Sample code S-1 was obtained by washing the PAA solution with ethyl ether (EE, Fisher Scientific) and a yellow precipitate was obtained. The precipitate was dissolved again in NMP. After filtering the undissolved residue, the solution was further precipitated with EE for 12 h. The precipitate was dried under vacuum at 25°C for 12 h.

To obtain samples S-2 and S-3, the PAA solution was coated on a glass plate, and the NMP was allowed to evaporate in a vacuum oven at controlled drying temperature and drying time (Table I). The solvent contents of samples S-1, S-2, and S-3, as measured by TGA, were NMP/PI = 4.06, 3.49, and 0.81 (molar ratio), respectively.

### Instrumentation

Thermogravimetric analysis (TGA) was carried out with a Perkin-Elmer TGA-7/7900 thermogravimetric analyzer, scanning from 30 to 450°C, with scanning rates varied from 2°C/min to 50°C/min. Furthermore, differential scanning calorimetry (DSC) data were obtained with a DuPont DSC-910/9900 thermal analyzer. Scanning rates ranged from 2 to 40°C/min, scanning from 25 to 400°C. Sample weight for both DSC and TGA was about 8.0 mg.

To obtain the reaction enthalpy for the imidization  $\Delta H_i$  from DSC, the PAA solution was first dried *in situ* in the DSC pan at several elevated temperatures (130, 135, 140, 150, and 170°C, respectively) for 10 min. This was to ensure that the NMP solvent was removed from the PAA solution so that

only enthalpy accounting for the imidization process was measured. The dried PAA was then scanned from room temperature to 400°C at a scanning rate of 10°C/min.

The kinetics of imidization were characterized by Fourier transform infrared spectroscopy (FTIR, Bio-Rad FTS-40) using potassium bromide (KBr) plates. The PAA solution was first coated on several KBr plates and dried at 85°C for 30 min, with a final NMP/PI = 3.5, molar ratio. The sample plates were then moved to a programmable temperature controller (Nabertherm C-19) with a heating rate of 10°C/min, from 85 to 400°C. For each 10°C interval, one of the KBr plates was removed from the oven, quickly quenched in liquid nitrogen, and measured by FTIR with a resolution of 4 cm<sup>-1</sup>, scanning from 400 to 4000 cm<sup>-1</sup>. The spectrum was obtained with the average of 64 scans.

## RESULTS AND DISCUSSION

### Complexation of NMP and PAA

#### Thermogravimetric Analysis

During a temperature sweep by TGA at heating rates from 2 to 50°C/min, sample S-1 displays a large weight loss of about 50% of the original weight (Fig. 2). Worthy of note in Figure 2 is that below a heating rate of 10°C/min, approximately 90% of the complexed NMP in sample S-1 is lost as the temperature reaches 200°C, while only 50% of the complexed NMP still remains in sample S-1 at 200°C when the heating rates are above 10°C/min. The amount of NMP remained in sample S-1 should determine the effect of subsequent plasticization when imidization begins at a higher temperature. Thus, a too low heating rate will not help the imidization.

When the derivative (the slope) of the weight loss curves in Figure 2 is taken (derivative thermogravimetric, DTG) and plotted versus temperature as shown in Figure 3, it is noted that the weight loss depends strongly on the heating rate. The temperature for the highest weight loss ( $T_m$ ) increases

**Table I** Preparation of Polyamic Acid Used in This Study

Sample Code	Drying Method	Drying Temp. (°C)	Drying Time (h)	NMP/PI (molar ratio)
S-1	EE extracted	25	12	4.06
S-2	Vacuum dried	25	46	3.49
S-3	Vacuum dried	96	1.25	0.81

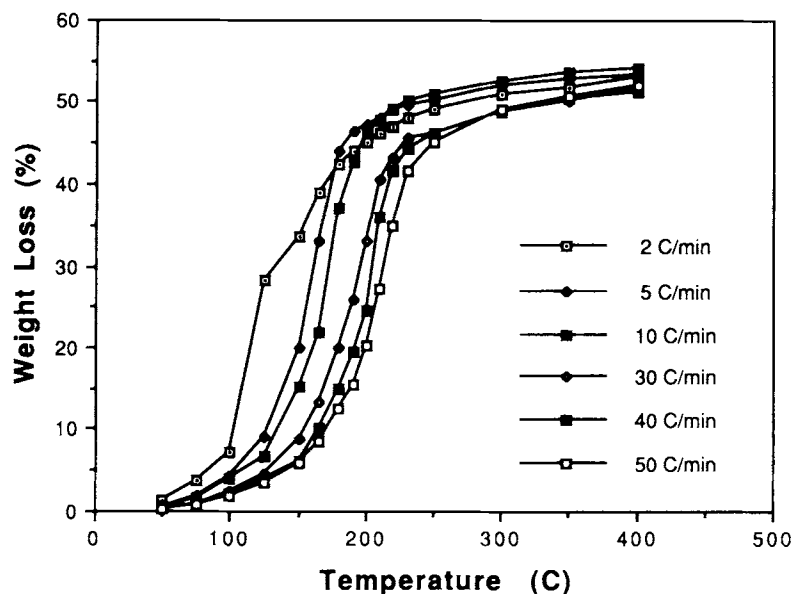


Figure 2 TGA curves of sample S-1 at six heating rates.

with increasing heating rate. Although minor fluctuations occur before the appearance of the major decomplexation peak (Fig. 3), in general there is only one major decomplexation for all the heating rates. The one-stage decomplexation process indicates that the complex formation between NMP and

PAA is not the same as in the model compound studied by other researchers.<sup>3</sup> This may be attributed to the chemical structure of the PAA molecules, which is far more complicated than the relatively simple diamic acid molecule. Therefore, spatial constraints may play a role in hindering the decom-

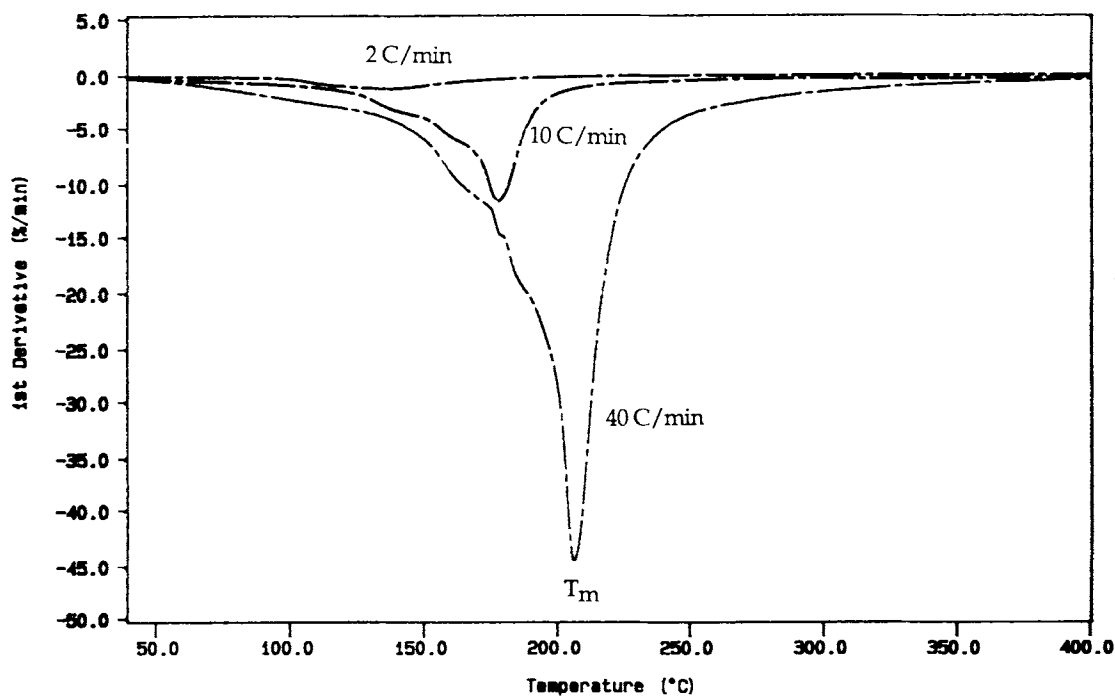


Figure 3 DTG curves of sample S-1 at three heating rates.

plexation process of the first two NMP molecules attached to the amide groups, which are decomplexed prior to the decomplexation of the other two NMP molecules attached to the acid groups in the diamide acid model compound.

### Estimation of Activation Energy of Decomplexation

Several methods for the estimation of the activation energies from TGA have been reported.<sup>7</sup> For a chemical reaction where the function of the extent of reaction  $\sigma$ ,  $f(\sigma)$ , is unknown, the reaction rate with the Arrhenius-dependent rate constant  $k = Z \exp(-E/RT)$ , can generally be expressed as

$$\begin{aligned} d\sigma/dT &= k(dt/dT)f(\sigma) \\ &= (Z/\lambda)\exp(-E/RT)f(\sigma) \quad (1) \end{aligned}$$

where  $\lambda (= dT/dt)$  is the heating rate,  $Z$  is the frequency coefficient,  $E$  is the activation energy,  $R$  is the gas constant, and  $T$  is the temperature. Assuming that there exists an analytical form of  $f(w)$  and without a definition of  $f(w)$ , Carroll and Manche<sup>8</sup> adopt Eq. (1) and offer the following equation for TGA:

$$\begin{aligned} \ln[\lambda(-dw/dT)] &= \ln(X) \\ &= \ln[Zf(w)] - E_d/RT \quad (2) \end{aligned}$$

where  $w$  is the weight loss and  $E_d$  is the activation energy of decomplexation. The derivative  $dw/dT$

can be obtained from DTG data. Thus, a plot of  $\ln(X)$  versus  $1/T$ , for a given value of  $w$  measured at several heating rates, will lead to a value of  $E_d$ . A representative plot based on this method is constructed in Figure 4 for a constant weight loss conversion of 50% at several heating rates. The kinetics of the decomplexation process can be characterized by a constant activation energy estimated from the slope of the solid line in Figure 4. Together with similar plots at other conversions, as summarized in Figure 5, an average value of  $E_d = 150$  kJ/mol is obtained. Note that a large deviation of  $E_d$  at 20% conversion is observed and is excluded from the average value. Regardless of the different conversions, the value of  $E_d$  are very close (with only 4% deviation) except the one based on the 20% conversion. This further confirms that the decomplexation process is a one-stage process (compared to Fig. 3).

Since the weight loss data obtained from TGA can only be referred to the decomplexation process, we proceed to use DSC in order to explore the effect of the decomplexation on the cure kinetics of imidization.

### Decomplexation and Imidization

#### Differential Scanning Calorimetry

The imidization process is also strongly affected by the heating rate. Figure 6 shows the plots of heat flow versus temperature of sample S-1 (NMP/PI = 4.06/1.00, molar ratio) measured by DSC in the

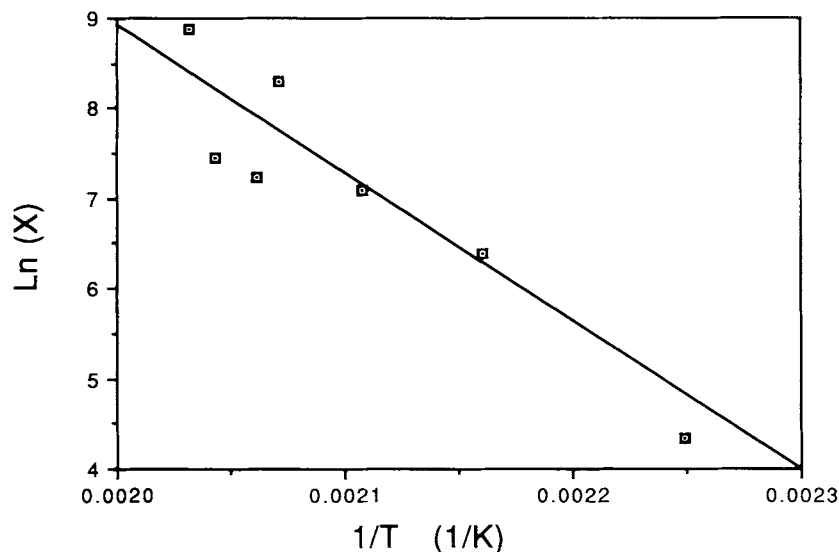


**Figure 4** Evaluation of activation energy of the decomplexation by the method of Carroll and Manche at a constant conversion of 50%.

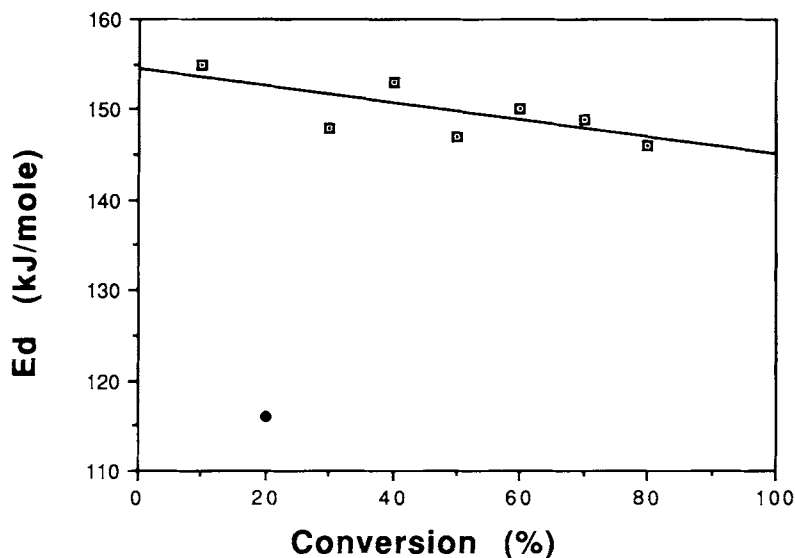


Figure 5 Activation energy of decomplexation at several conversions.

scanning mode with scanning rates varying from 5 to 40°C/min. For each scanning rate, there are generally two endothermic peaks. The first peak takes place between 140 and 170°C, which is attributed

mainly to the decomplexation of NMP molecules H-bonded to the amide and carboxylic groups. In addition, there is also minor imidization accomplished with this decomplexation. The second peak

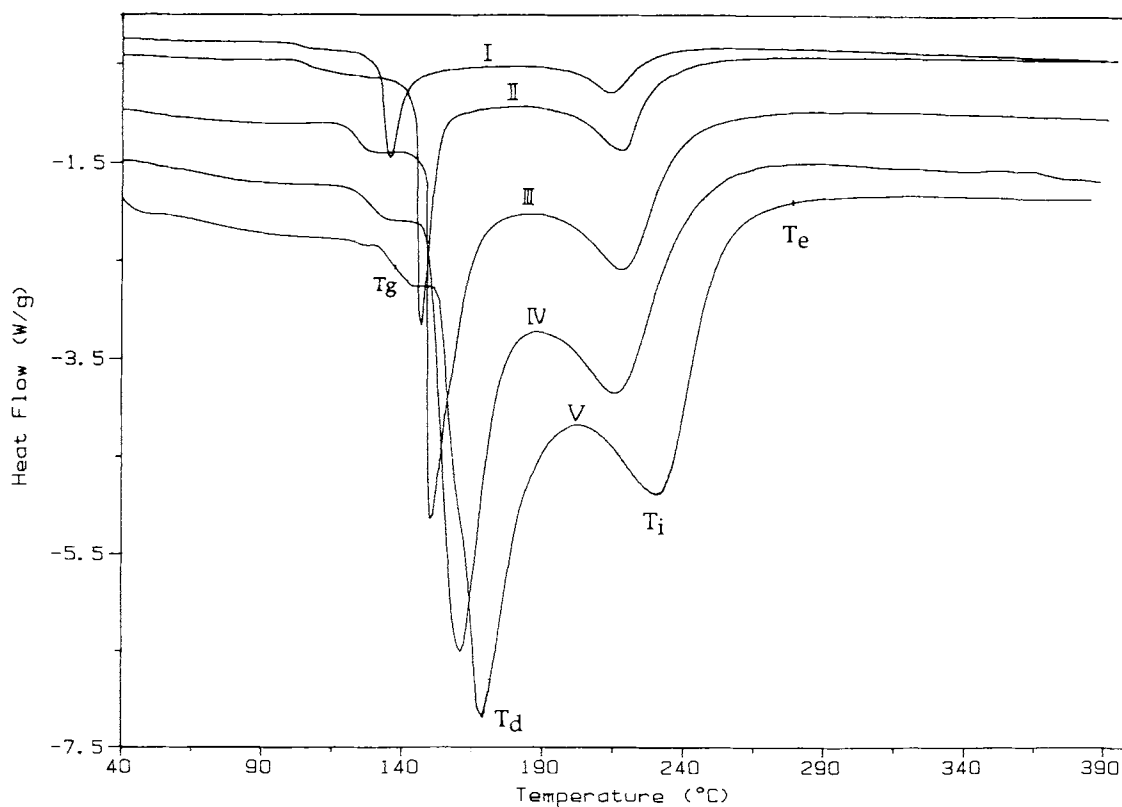
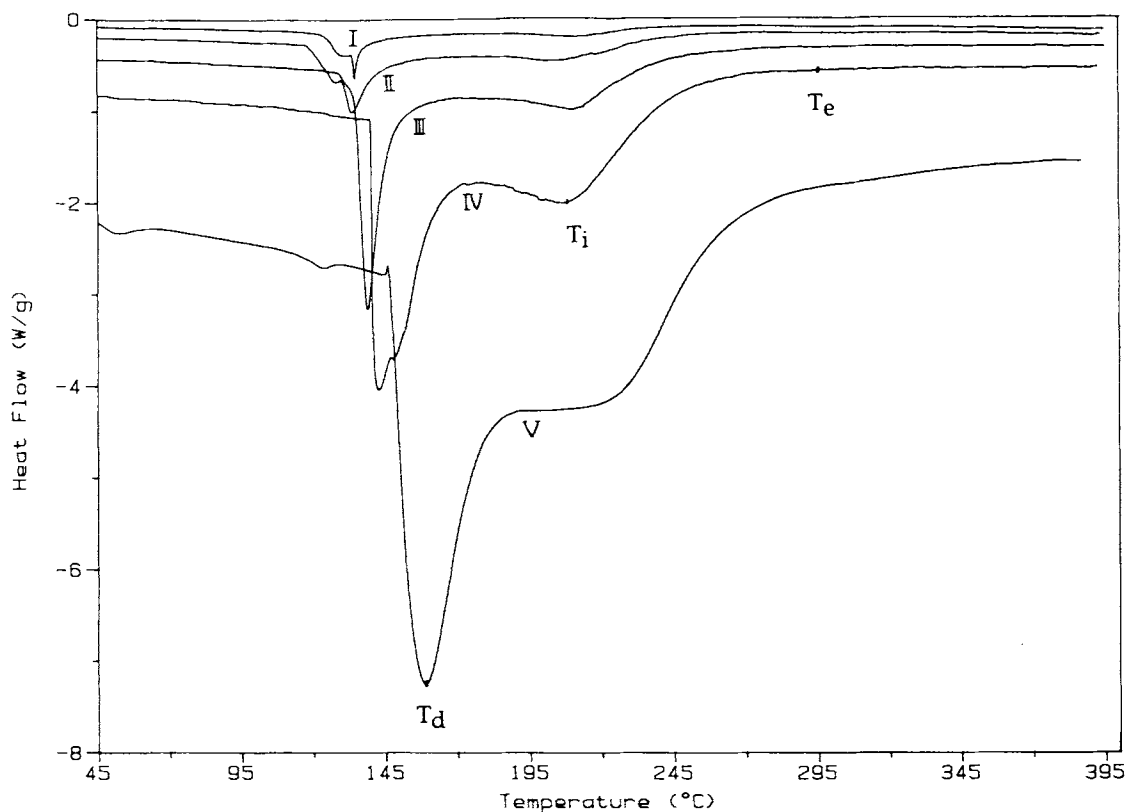


Figure 6 Heating-rate-dependent DSC curves of sample S-1. (I) 5°C/min; (II) 10°C/min; (III) 20°C/min; (IV) 30°C/min; (V) 40°C/min.



**Figure 7** Heating-rate-dependent DSC curves of sample S-2. (I) 2°C/min; (II) 5°C/min; (III) 10°C/min; (IV) 20°C/min; (V) 40°C/min.

takes place around 210°C, which is attributed mostly to the imidization resulted from dehydrative cyclization of amide and amino groups to form the imide rings.

It is also observed from Figure 6 that both the glass transition temperature of PAA ( $T_g$ ) and the peak temperature of the decomplexation ( $T_d$ ) increase with increasing scanning rate. On the other hand, the imidization peak ( $T_i$ ) does not increase with heating rate, but stays rather constant except at the higher heating rate of 40°C/min. The  $T_e$  peak, denoted as the end of imidization, also increases with increasing heating rate. The same trend can be observed for sample S-2 (NMP/PI = 3.49) and sample S-3 (NMP/PI = 0.81) (Figs. 7 and 8).

For sample S-2 in Figure 7, the endothermic peaks  $T_i$  are not as strong as those in Figure 6. For sample S-3 in Figure 8, with only 0.81 molar ratio of NMP molecules, drastic changes in heat flow profiles are observed. The decomplexation peak ( $T_d$ ) moves to a lower temperature around 100°C. This endothermic peak is characteristic not only of the solvent decomplexation but also of the anhydride formation due to thermal degradation of PAA molecules into

anhydride and amino group.<sup>3</sup> This anhydride formation is reversible. Therefore, upon further heating, the anhydride groups and amino groups recombine again and eventually become imide groups at higher temperatures. The imidization starts also at lower temperatures for sample S-3 and expands to quite a broad temperature range of about 100°C. Figure 9 gives a more detailed comparison among three PAA samples at a heating rate of 10°C/min.

The characteristic peak temperatures of all three samples are summarized in Figure 10. It is observed that the imidization process takes place after the decomplexation process. The decomplexation temperature  $T_d$  increases with increasing heating rate (excluding sample S-3 at high heating rates). The imidization process is less sensitive to the heating rate. Except for sample S-3 at low heating rates, all the  $T_i$ 's remain fairly constant. This is primarily due to the presence of the free NMP molecules, which help to plasticize the PAA once they are decomplexed. The amount of free NMP molecules and their duration in the PAA decide the extent of plasticization. On the other hand,  $T_e$  increases with increasing heating rate. This is mainly due to faster

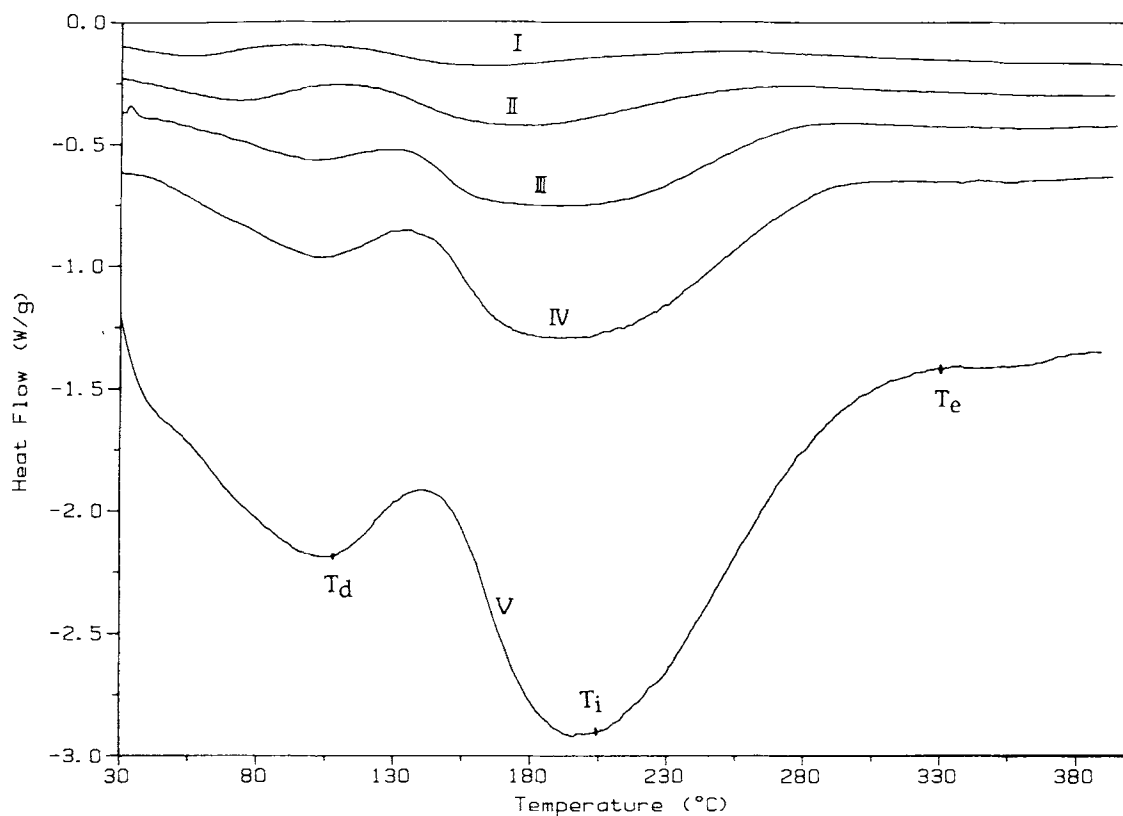


**Figure 8** Heating-rate-dependent DSC curves of sample S-3. (I) 2°C/min; (II) 5°C/min; (III) 10°C/min; (IV) 20°C/min; (V) 40°C/min.

evolution of NMP molecules leaving PAA, thus reducing their capability of plasticization and resulting in a higher  $T_e$ .

It is also observed from Figure 10 that as the solvent content in PAA decreases,  $T_d$  moves to lower temperature and  $T_e$  moves to higher temperature.

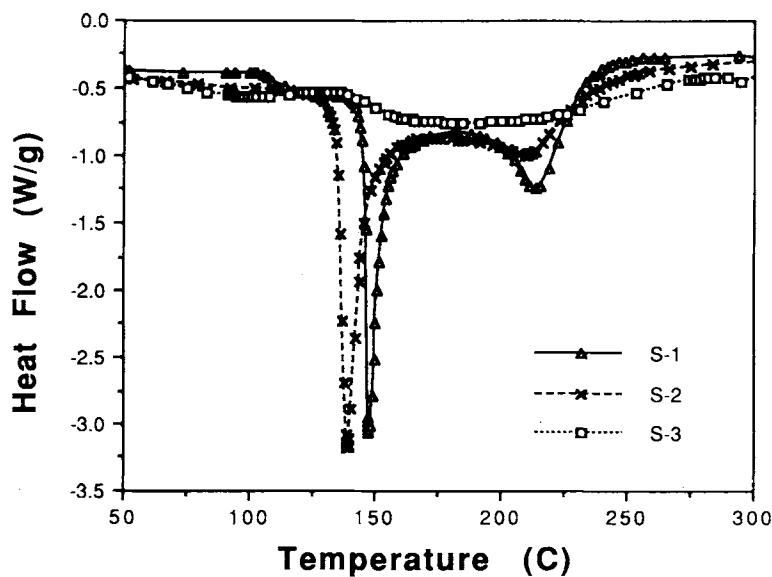


**Figure 9** DSC curves for three PAA samples of different solvent content.



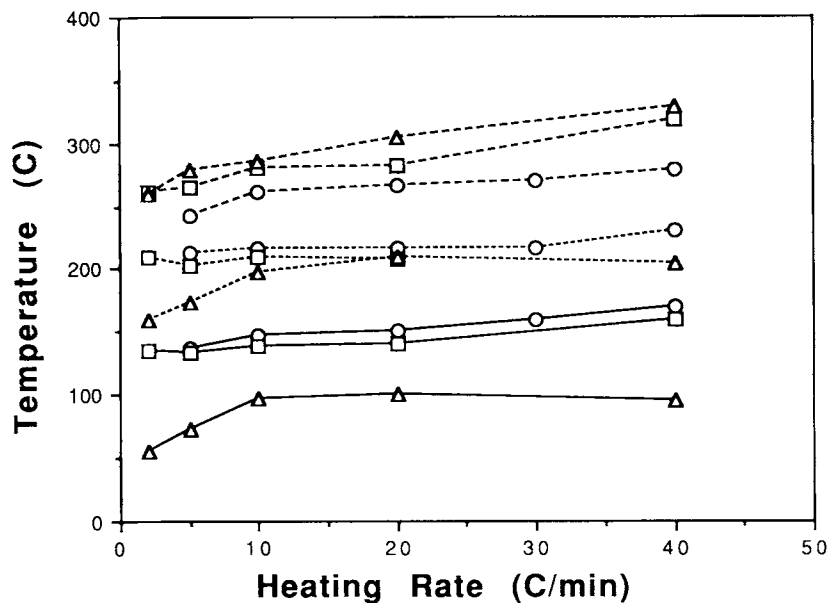


**Figure 10** Characteristic temperatures of DSC curves of NMP-complexed PAA plotted vs. heating rate. (—):  $T_d$ ; (----):  $T_i$ ; (---):  $T_e$ ; (○): sample S-1; (□): sample S-2; (△): sample S-3.

The former is attributed to the increasing anhydride formation and the latter is attributed to the decreasing effect of plasticization. On the other hand,  $T_i$  is relatively insensitive to the changes of solvent content, except at low heating rates for sample S-3. The results from Figures 6 to 10 suggest that over-drying PAA results in a prolonged imidization process due to lack of plasticization. Accordingly, the

imidization is retarded in the absence of NMP molecules.

#### Estimation of Reaction Enthalpy by DSC

In order to assess quantitatively the heat evolved for the decomplexation and the imidization processes, sample S-1 was first dried *in situ* in the DSC

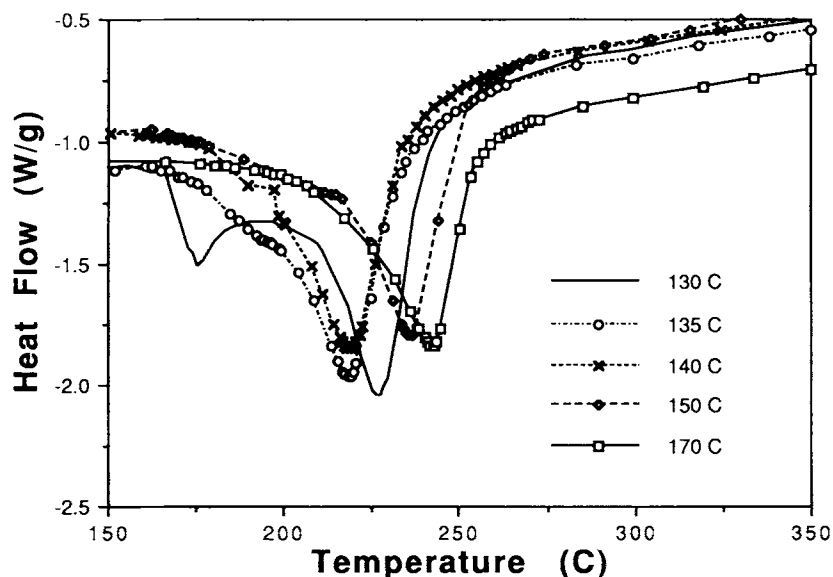


**Figure 11** Scanning DSC curves of PAA isothermally dried at five elevated temperatures.

**Table II** Enthalpy of Imidization

Iso Temp. (°C)	$T_0^a$ (°C)	$T_i$ (°C)	$\Delta H_i$ (J/g)
135	196	219	289
140	193	219	296
150	210	237	282
179	212	245	277

<sup>a</sup> Temperature at which imidization starts.

pan for 10 min at constant elevated temperatures, which are generally higher than normally practiced in the commercial applications, and then they were scanned from 25 to 400°C at a heating rate of 10°C/min (Fig. 11).

It is noted from Figure 11 that, except for the one at 130°C, only the imidization peak appears and the decomplexation peak diminishes completely by this high-temperature drying. This allows one to calculate the molar enthalpy of imidization,  $\Delta H_i$ , from Figure 11. Thus, an average of  $\Delta H_i = 286$  J/g (114 kJ/mol) is obtained as shown in Table II. Figure 11 shows that sample S-1 dried at 130°C exhibits a residual decomplexation peak, suggesting it is not completely solvent free; therefore, it is excluded. Also displayed in Figure 11 and Table II is the increasing  $T_0$  (temperature at which imidization starts) and  $T_i$  with increasing isothermal drying temperature.

The molar enthalpy  $\Delta H$  of the PAA solution measured from Figure 6 (for sample S-1) includes the enthalpy of both decomplexation and imidization processes, i.e.,  $\Delta H = \Delta H_i + \Delta H_d$ , where  $\Delta H_d$  is the enthalpy for the decomplexation process. It may be observed that the value of  $\Delta H$  decreases with increasing heating rate, but the deviation is within only 5%. An average value of  $\Delta H = 418$  J/g is obtained (Fig. 12). Subtracting  $\Delta H_i$  from  $\Delta H$  yields directly  $\Delta H_d$ . Theoretically, there is 50% by weight of NMP present in the 4/1 complex (sample S-1). This gives an estimated value of  $\Delta H_d = 53$  kJ/mol NMP (calculations based on weight ratio), which is in good agreement with the reported data of 55 kJ/mol NMP for the second decomplexation in the model compound studied.<sup>3</sup>

### Kinetic Measurements of Imidization

#### Qualitative Spectrum Assignments by FTIR

Generally speaking, kinetic information on imidization derived from DSC data is affected by the decomplexation process, owing to the presence of solvent molecules. To obtain more accurate and detailed information about the imidization kinetics without solvent interference, we used FTIR by preparing a "dry" thin film of PAA solution. Prior to FTIR measurements, the thin PAA film was dried at 85°C for 30 min with final NMP/PI = 3.5, equal to that in sample S-2.

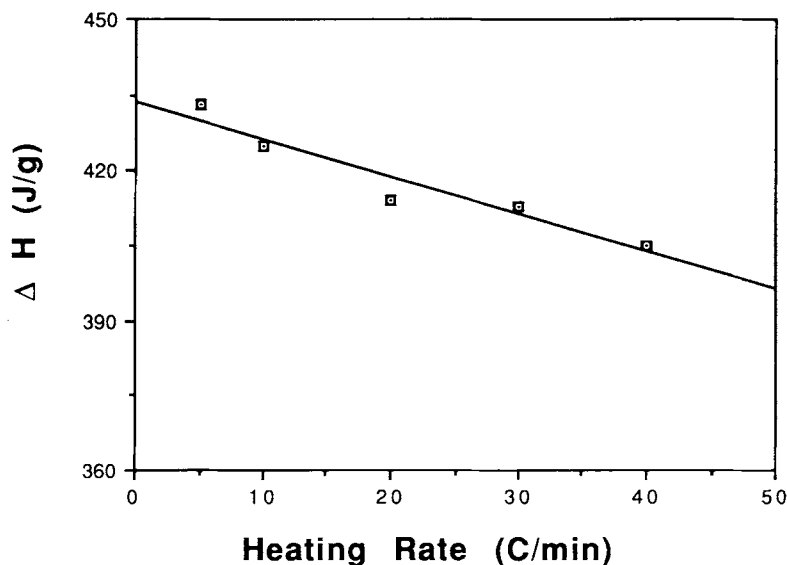


**Figure 12** Reaction enthalpy (including decomplexation and imidization) measured from DSC curves in Figure 6 for sample S-1 at several heating rates.

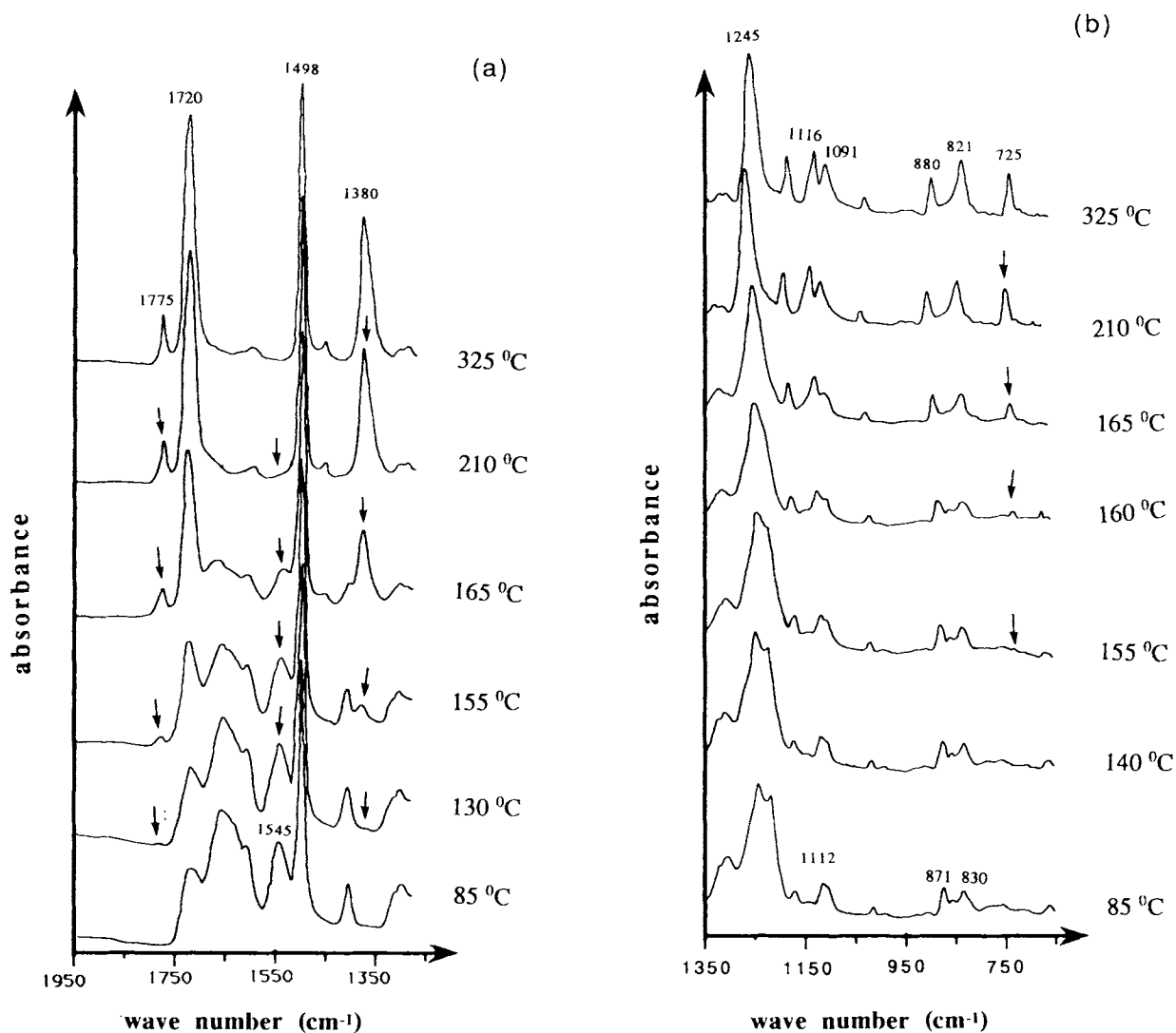


**Figure 13** FTIR spectra showing the characteristic peak changes during the curing of PAA film at several temperatures. (a) 1950–1250  $\text{cm}^{-1}$ ; (b) 1350–650  $\text{cm}^{-1}$ .

The reaction kinetics of polyimide resins have been investigated using FTIR by various authors.<sup>9–11</sup> The FTIR analysis is based on the peak change of functional groups or characteristic linkages during the reaction period. Therefore, more than one peak may change when the imidization takes place. In Figure 13 the FTIR spectra is shown for the formation of polyimide from PAA solution during a temperature scan from 85 to 400 °C at a heating rate of 10 °C/min. In principle, the imide peak at 1775  $\text{cm}^{-1}$  (C=O symmetrical stretching), 1720  $\text{cm}^{-1}$  (C=O coupled stretching), and the amide peak at 1545  $\text{cm}^{-1}$  (amide II) can all be followed during imidization reaction in which amide groups are consumed and imide groups are formed. Other spectral

features include the decreasing band of NMP at 1408  $\text{cm}^{-1}$  (NMP  $\text{CH}_2$  bending); the broad and less obvious change of amide peak at 1664  $\text{cm}^{-1}$  and 1602  $\text{cm}^{-1}$ , and the minor change of cyclic anhydride peak at 1303  $\text{cm}^{-1}$ . The 1408  $\text{cm}^{-1}$ , indicative of the NMP molecules, disappears after the temperature reaches about 165 °C. The present peak assignments, summarized in Table III, are in general agreement with those obtained in literature.<sup>3,9–11</sup>

#### Quantitative Description of Cure Kinetics by FTIR

To study the imidization kinetics of the polyimide resins, we chose the peak of aromatic ring stretching at 1498  $\text{cm}^{-1}$  as the internal standard and adopted

**Table III FTIR Spectrum Assignment and Their Temperature Dependency**

Peak (cm <sup>-1</sup> )	Peak Intensity <sup>a</sup>	Assignment	Ref.
1775	↗	C=O symmetrical stretching	5
1720	↗	C=O stretching (coupled)	5
1664	↘	Amide II	5
1602	↘	Amide II	9
1545	↘	Amide II	3
1498	No change	Aromatic ring stretching	3
1408	↘	NMP CH <sub>2</sub> bending	3
1380	↗	Imide ring C—N stretching	5
1303	↘	Cyclic anhydride	5
1245	No change	Aromatic ether C—O stretching	12
1216	↘	Acid group	3
725	↗	Cyclic C=O bending	5

<sup>a</sup> ↗: increasing with increasing temperature; ↘: decreasing with increasing temperature.

the peak height method to calculate the amount of the appearing imide groups formed in the reactive system according to

$$\alpha = (D/D^*)_{T,\text{imide}} / (D/D^*)_{O,\text{imide}} \quad (3)$$

where  $\alpha$  represents the conversion (extent of imidization or extent of cure),  $D^*$  is the peak height

of the internal standard at 1498 cm<sup>-1</sup>, and  $D$  is the imide peak (1775, 1720, 1545, 1380, and 725 cm<sup>-1</sup> in this study). Subscript  $O$  and  $T$  indicates reaction at initial temperature and at temperature  $T$ , respectively. The relatively small peak at 1012 cm<sup>-1</sup> characteristic of the aromatic vibration was frequently used in the literature as the internal standard. We prefer to use the 1498 cm<sup>-1</sup> for more accurate estimation of the kinetic information. The conversion  $\beta$  of the disappearing amide group defined as

$$\beta = 1 - (D/D^*)_{T,\text{amide}} / (D/D^*)_{O,\text{amide}} \quad (4)$$

should be used to indicate the extent of cure. Theoretically,  $\alpha = \beta$ . Plots of conversion versus temperature for five characteristic absorption peaks are shown in Figure 14. The results are quite consistent for all five peaks, except the peak at 725 cm<sup>-1</sup>.

In general, there are four stages during the entire imidization process. Up to a temperature of 150°C, less than 20% of amide groups (except the 725 cm<sup>-1</sup> curve) have reacted to give imide groups, and the reaction is slow. Most of the imidization takes place between 150 and 180°C, and the conversion may be as high as 90%. The imidization process is completed after temperature is further raised to 250°C. Finally, above 250°C, a lowering of final conversion back to 80% is observed.

The curve of 725 cm<sup>-1</sup> in Figure 14 exhibits a higher conversion in the early stage of imidization.

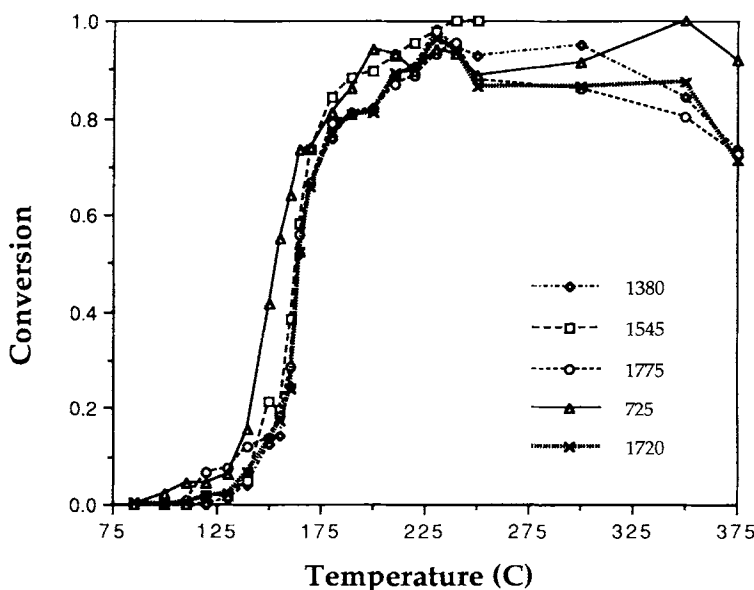


**Figure 14** Plots of conversion vs. temperature for five characteristic peaks (in cm<sup>-1</sup>) from Figure 13.

In addition, the curves 1775, 1720, and 1380  $\text{cm}^{-1}$  show a maximum of about 95% at ca. 225°C and gradually reduce to about 80% when the temperature rises above 250°C. This could be attributed to configurational changes during heating<sup>12</sup> and densification at high temperatures.<sup>6,13</sup> For the configurational changes, the C=O groups in the imide rings are forced to be directly opposite each other. At a temperature below 250°C, the C=O bonds are at an angle to the chain axis because of steric constraints. Therefore, there is no change in dipole moment during symmetric stretching. Since infrared spectroscopy is a measure of the dipole moment, in the case where there is no dipole moment change, no absorption in the IR is expected. On the other hand, the densification process may result from an increase in the chain mobility at high temperatures, which permits a molecular packing process (ordering) to occur. This ordering process has been observed by an increase of the storage modulus in dynamic mechanical testing.<sup>6</sup>

## CONCLUSIONS

We have demonstrated in this study the effect of solvent NMP on the curing of polyimide resins synthesized from PMDA and ODA using TGA, DSC, and FTIR. Results from TGA showed that there was only one major decomplexation peak observed. The one-stage decomplexation process suggested that the complex formation of NMP and PAA was not the same as the model compound studied by others. An average value of 150 kJ/mol for the activation energy of the decomplexation process was obtained. Our DSC results indicated that the imidization process took place only after the decomplexation process; the decomplexation was strongly affected by the heating rate; and the imidization was less sensitive to the heating rate. Over-drying PAA resulted in prolonged imidization due mainly to the lack of plasticization by decomplexed NMP. The estimated enthalpy of imidization and that of decomplexation were 114 kJ/mol and 53 kJ/mol NMP, respectively. From FTIR analysis, the results indicated that there were four stages during the entire imidization process. Up to a temperature of 150°C, less than 20% of amide groups have reacted to give imide groups, and the reaction was slow. Most

of the imidization took place between 150 and 180°C and the conversion might be as high as 90%. The imidization process was completed after the temperature was further raised to 250°C. Above 250°C, the reverse reaction became more significant (due probably to configurational and packing preference) and resulted in a lowering of final conversion back to 80%.

This work was supported in part by National Science Council of the Republic of China (NSC80-0405-E-110-06) and a grant from China Steel Corporation. The authors wish to thank Mr. T. L. Chen for helping the TGA experiments.

## REFERENCES

1. E. Sugimoto, *IEEE Electrical Insulation Magazine*, **5**, 15 (1989).
2. M. I. Bessonov, M. M. Koton, V. V. Kudryavtsev, and L. A. Laius, *Polyimides, Thermally Stable Polymers*, Chap. 4, trans. by L. V. Backinowsky, M. A. Chlenov, and W. W. Wright, Consultants Bureau, New York, 1987.
3. M.-J. Brekner and C. Feger, *J. Polym. Sci. Polym. Chem. Ed.*, **25**, 2005 (1987).
4. M.-J. Brekner and C. Feger, *J. Polym. Sci. Polym. Chem. Ed.*, **25**, 2479 (1987).
5. M. I. Bessonov, M. M. Koton, V. V. Kudryavtsev, and L. A. Laius, *Polyimides, Thermally Stable Polymers*, Chap. 1, trans. by L. V. Backinowsky, M. A. Chlenov, and W. W. Wright, Consultants Bureau, New York, 1987.
6. C. Feger, *Polym. Eng. Sci.*, **29**, 347 (1989).
7. E. A. Turi, ed., *Thermal Characterization of Polymeric Materials*, Academic Press, New York, 1981.
8. B. Carroll and E. P. Manche, *Thermochim. Acta*, **3**, 449 (1972).
9. A. N. Krasovskii, N. P. Antonov, M. M. Koton, K. K. Kalnin'sh, and V. V. Kudryavtsev, *Polym. Sci. U.S.S.R.*, **21**, 1038 (1980).
10. L. A. Laius, M. I. Bessonov, Ye. V. Kallistova, N. A. Adrova, and F. S. Florinskii, *Vysokomol. Soyed.*, **A9**, 2185 (1967).
11. R. Osredkar, *Microelectron. Reliab.*, **28**, 599 (1988).
12. R. W. Snyder, C. W. Sheen, and P. C. Painter, *Appl. Spectrosc.*, **42**, 503 (1988).
13. N. Takahashi, D. Y. Yoon, and W. Parrish, *Macromolecules*, **17**, 2583 (1984).

Received October 24, 1991

Accepted January 20, 1992